

Primljen / Received: 30.6.2020.

Ispravljen / Corrected: 14.8.2020.

Prihvaćen / Accepted: 7.10.2020.

Dostupno online / Available online: 10.1.2021.

Flexural response of SF concrete beams internally reinforced with different types of FRP bars

Authors:



Assoc.Prof. **I.A. Sharaky**, PhD. CE
Taif University, Saudi Arabia
Department of Civil Engineering
Zagazig University, Egypt
Faculty of Engineering, Department of Materials
ibm_attia@zu.edu.eg



Prof. **H.K. Shehab Eldin**, PhD. CE
Zagazig University, Egypt
Faculty of Engineering, Department of Materials
hshehab@yahoo.com



Mohamed M. Shehata, MSc. CE
Zagazig University, Egypt
Faculty of Engineering, Department of Materials
mohamadyshata74@gmail.com



Assoc.Prof. **Heba A. Mohamed**, PhD. CE
Zagazig University, Egypt
Faculty of Engineering, Department of Materials
hebawahbe@yahoo.com

Corresponding author

Original scientific paper

I.A. Sharaky, H. K. Shehab Eldin, Mohamed M. Shehata, Heba A. Mohamed

Flexural Response of RC beams cast with normal and steel fibre concrete internally reinforced with various types of FRP bars

Fibre Reinforced Polymer (FRP) bars can be used as an alternate for reinforcing bars to avoid corrosion of steel. Samples of reinforced concrete beams cast with normal or steel fibre concrete (SFC), internally reinforced with Glass Fibre Reinforced Polymer (GFRP) or steel bars, are prepared and tested in this paper. Experimental results show that compressive strength of concrete increases with an increase in steel fibre (SF) ratio used in this study (from 0% to 1.5%). Also, the beams reinforced with GFRP bars have a lower initial stiffness and higher ductility than those reinforced with steel bars.

Key words:

reinforced-concrete beams, fibre reinforced polymers, steel fibres, CFRP, GFRP, AFRP

Izvorni znanstveni rad

I.A. Sharaky, H. K. Shehab Eldin, Mohamed M. Shehata, Heba A. Mohamed

Savijanje AB greda od običnog betona i betona s čeličnim vlaknima armiranih različitim vrstama FRP šipki

Šipke od vlaknima armiranih polimera (FRP) mogu se koristiti kao zamjena za čelične šipke da bi se izbjegla korozija čelika. U ovom radu su pripremljeni i ispitani uzorci armiranobetonskih greda od običnog betona i betona s čeličnim vlaknima (SFC) armirani šipkama od staklenih vlakana, armiranih polimera (GFRP) ili čeličnim šipkama. Rezultati ispitivanja pokazali su da se tlačna čvrstoća betona povećala s povećanjem omjera čeličnih vlakana (SF) koji su korišteni u ovom istraživanju (od 0 % do 1,5 %). Jednako tako, grede armirane GFRP šipkama imale su nižu početnu krutost i veću duktilnost nego one armirane čeličnim šipkama.

Ključne riječi:

armiranobetonske grede, vlaknima armirani polimeri, čelična vlakna, CFRP, GFRP, AFRP

Wissenschaftlicher Originalbeitrag

I.A. Sharaky, H. K. Shehab Eldin, Mohamed M. Shehata, Heba A. Mohamed

Biegen von Stahlbeton-Trägern aus normalem Beton und Beton mit Stahlfasern, die mit verschiedenen Arten von FK-Stäben bewehrt sind

Faserverstärkte Polymerstäbe (FK) können als Ersatz für Stahlstäbe verwendet werden, um Stahlkorrosion zu vermeiden. In dieser Arbeit wurden Proben von Stahlbetonbalken aus gewöhnlichem Beton und Stahlfaserbeton (SFB) hergestellt und getestet, die mit Glasfaserstäben, verstärkten Polymeren (GFK) oder Stahlstäben bewehrt waren. Die Testergebnisse zeigten, dass die Druckfestigkeit des Betons mit zunehmendem Anteil der in dieser Studie verwendeten Stahlfasern (SF) zunahm (von 0 % auf 1,5 %). Ebenso hatten mit GFK-Stäben bewehrte Träger eine geringere Anfangssteifigkeit und eine höhere Duktilität als mit Stahlstäben bewehrte Träger.

Schlüsselwörter:

Stahlbetonbalken, faserverstärkte Polymere, Stahlfasern, CFK, GFK, AFK

1. Introduction

Fibre Reinforced Polymer (FRP) bars are currently utilised as longitudinal bars and stirrups for reinforcing various concrete structures such as marine structures, bridge decks, tunnels, parking structures, and water treatment plants. Due to FRP advantages compared to steel bars (high strength to weight ratio and durability), the use of FRP instead of steel as internal reinforcement for concrete elements has become increasingly common, especially in North America, as a means to avoid steel corrosion problems. Flexural behaviour of RC beams reinforced with FRP bars is investigated in previous researches [1-10]. Flexural ductility of RC elements with steel bars is calculated as the ratio of ultimate displacement to displacement at steel yield, while in the case of RC elements reinforced with FRP bars it can be calculated in a number of ways [11-13]. Generally, it has been adduced that the concrete properties are considered the basic factor affecting the ductility of RC beams with FRP bars rather than the FRP properties.

A lot of research has been performed on the application and mechanical properties of reinforced concrete beams with GFRP (Glass Fiber Reinforced Polymer - GFRP), such as their flexural behaviour, bond properties, fracture performance, and durability [14-20]. The most important results gained in the scope of these research activities have revealed that the deflection at mid-span and crack width decrease significantly with an increase in reinforcement ratio. Also, by increasing the reinforcement ratio from μ_b to $1.7 \mu_b$ and from μ_b to $2.7 \mu_b$, respectively, (μ_b : is the reinforcement ratio at balanced condition) an increment of 47 % and 97 % in ultimate load was registered [19]. The bond stress was inversely proportional to the bar diameter and embedment length of GFRP bars. In addition, as expected, the headed-end GFRP bars had higher pullout strength than that of the straight-end bars.

Omar et al. [21] studied flexural response of RC beams cast with normal concrete (NC) and high strength concrete (HSC). The test results indicated that an increase in the FRP reinforcement ratio influenced the service moment rather than the resistance moment of tested beams. Also, a decrease in the FRP bar spacing increased the service moment, while an increase in concrete strength increased the load capacity of tested beams. Moreover, the concept of deformability produced higher ductility index than the concept of energy. On the other hand, seven geopolymers-concrete beams with various ratios and arrangements of GFRP-to-steel reinforcement were studied [22]. The experimental results demonstrated that hybrid beams had better ductility and serviceability than geopolymer concrete beams reinforced with GFRP bars only. Also, hybrid beams exhibited up to 15 % higher strength compared to geopolymer concrete beams reinforced with GFRP bars only. Wen et al. [23] studied the effects of GFRP shear reinforcement ratios, and of compression and tensile reinforcement, on

the energy dissipated in RC beams. This study shows that the corrosion resistance and strength of GFRP bars can be absolutely exploited by adding FRP for stirrup and tensile reinforcement. When adding GFRP bars in the compression zone, the strain energy values, and the corresponding ratios, displayed consistent upward orientations with an increase in the ratio of GFRP reinforcement.

The experimental results of Araba and Ashour [24] revealed that an increase in the load carrying capacity with an increase in the GFRP reinforcement ratio resulted in low ductility. Moreover, due to FRP linear-elastic response up to failure, continuous RC beams with FRP bars showed lower ability to redistribute stresses among critical sections, compared to beams reinforced with steel bars [25-27]. Moreover, Bischoff and Gross [28, 29] demonstrated that a sudden loss of stiffness at cracking affected the deflection and post-cracking behaviour. Mousavi et al. [30] investigated deflection of GFRP-RC beams, and alleged that the low elastic modulus (E) of GFRP bars causes sudden loss of concrete stiffness. In addition, the bond coefficient and elastic modulus (E) of FRP were the main factors manipulating the GFRP-RC beam behaviour. Due to the low values of E and shear modulus (G) of FRP, the arrangement of GFRP profiles with concrete features to resist high loads using a stiffer hybrid structure was a good recommended solution [31-41].

From the above review, it can be concluded that most previous studies focused on the analysis of RC beams with GFRP bars. On the other hand, the use of SF and FRP for RC beams is still limited. In this paper, the flexural behaviour and ductility of concrete beams reinforced with GFRP bars and steel fibre are studied experimentally. The type of internal reinforcement (steel and GFRP) and volume fraction of steel fibre (1 and 1.5 %) were studied with regard to flexural behaviour of RC beams. Furthermore, a non-linear finite element analysis using ANSYS program was conducted to study flexural behaviour of concrete beams reinforced with SF and with different types of FRP bars (glass, aramid and carbon bars).

2. Experimental Program

2.1. Material properties and mix proportions

The RC beams were tested with and without steel fibres. Based on most previous studies, the percentage of steel fibres (SF) ranged between 0 % and 2 % (i.e. 0, 0.5 %, 0.75 %, 1 %, 1.5, and 2 %). Yuanxun Zheng et al. [42] indicated that compressive strength increases faster when fibre content is less than 1 %, while the rate of compressive strength increase is slower when the fibre content is more than 1 % (e.g., 1.5 % and 2 %). That is why two percentages of SF (1 % and 1.5 %) were used in this study. The compressive and tensile strengths of concrete were obtained using standard

cubes (150 mm edge) [43], standard cylinders (150 × 300 mm) [44], respectively. The effect of SF on the concrete compressive and tensile strength will be discussed later. Experimentally obtained properties of steel bars [45] were: 390 MPa, 572 MPa, and 2×10^5 MPa, for yield strength, tensile strength, and modulus of elasticity, respectively. The GFRP bars were manufactured in Materials Laboratory of Zagazig University. Tensile tests were carried out on three specimens of GFRP bars [46]. Average properties obtained on these GFRP specimens were 596 MPa, 36.1 GPa, and 0.0165 for tensile strength, modulus of elasticity, and maximum strain, respectively. The stress-strain curve for steel bars and GFRP bars, as based on the above testing, is shown in Figure 1. Hooked end SFs 50 mm in length (Figure 2), with properties as summarized in Table 1, were used.

According to the fibre volume fraction, there are three concrete mixes that are obtained by changing the weight of SF, while the weights of other materials are kept constant. The quantities of materials used for the concrete mix are shown in Table 2. The percentage of fibre weight can be calculated using the following Eq. (1):

$$W_f = \frac{v_f \cdot D_f}{v_m \cdot D_m + v_f \cdot D_f} \quad (1)$$

where:

- W_f - percentage of fibres in the total weight of tested specimen
- v_f - fibre volume fraction (0 %, 1 % i 1.5 %)
- D_f - density of fibres (7.84×10^{-5} N/mm³)
- D_m - density of matrix
- v_m - matrix volume fraction ($v_m = 100 - v_f$).

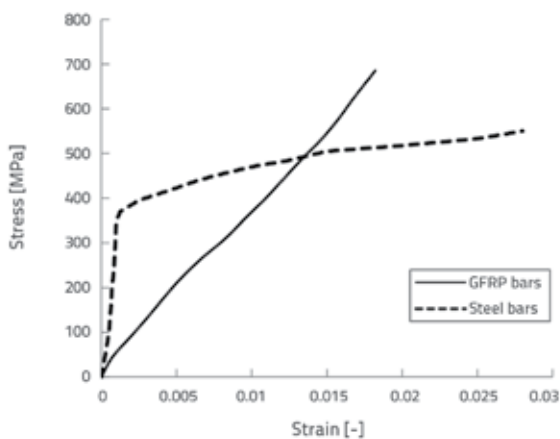


Figure 1. Stress-strain curve for steel and GFRP bars

Table 2. Mix proportions for 1 m³ concrete

Component	Cement	Water	Dolomit, No. 1 (Nominal size: 12.5 mm)	Dolomit, No. 2 (Nominal size: 20 mm)	Sand
Mass [kg]	360	195	600	600	640



Figure 2. Hooked end steel fibre

Table 1. Properties of steel fibre (from manufacturer)

Property	Value
Specific gravity [kN/m ³]	78.4
Tensile strength [N/mm ²]	800 – 1500 (1100)
Crimped height [mm]	2 - 3
Diameter [mm]	0.75
Length [mm]	50
Young's modulus [MPa]	2×10^5
Aspect ratio, Approx.	67

2.2. Characteristics of beams

A total of six concrete beams were cast and tested. Two types of concrete, normal concrete (NC) and SFC, were used to cast RC beams. All beams were 150 × 250 mm in cross section and 2000 mm in total length, as illustrated in Figure 3. The details about the tested beams are provided in Table 3. All the beams were reinforced in compression using two steel bars 12 mm in diameter. The shear reinforcement consisted of steel stirrups 8 mm in diameter, spaced at 130 mm intervals, for all tested beams (see Figure 3). The tensile reinforcement of the beams consisted of steel or GFRP bars with the reinforcing ratio of 0.66 %. The beam S0.OSF was cast with NC and reinforced with two steel bars 12 mm in diameter as tensile reinforcement (control beam, CB). The beam G0.OSF was cast with NC and reinforced in tension using two GFRP bars 12 mm in diameter to study the effect of internal tensile reinforcement on flexural behaviour and ductility of the beam (see Figure 4).

Table 3. Beam configuration and test variables

Beam, ID	Bottom Reinforcement	SF ratio [%]	Test variable
S0.0SF(CB)	Steel	0	Control
G0.0SF	GFRP	0	Reinforcement type
S1.0SF	Steel	1	SF ratio
G1.0SF	GFRP	1	Reinforcement type
S1.5SF	Steel	1.5	SF ratio
G1.5SF	GFRP	1.5	Reinforcement type

2.3. Test setup and Instrumentation

All beams were tested using four points loading (4PB) over an effective simply supported span of 1800 mm with a shear span of 600 mm (see Figure 5). The loading was stopped after the collapse bang was heard (i.e. after reinforcement fracture or concrete crushing) or after the load cell showed a big decrease in load results, with the load being less than 85 % of ultimate load. The beams were loaded at a rate of 0.06 kN/s.

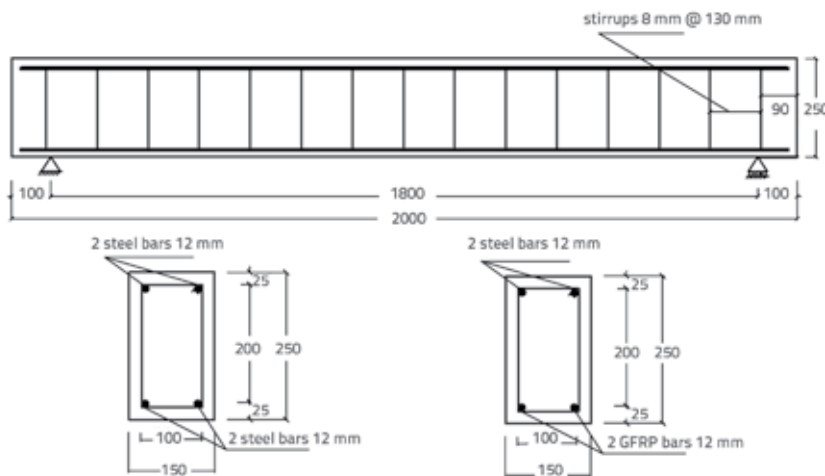


Figure 3. Dimensions and reinforcement details of tested beams (dimensions in mm)

To study the effect of SF on the RC beams with steel tensile reinforcement, two beams (S1.0SF and S1.5SF), having the same internal reinforcement as beam S0.0SF, were cast using SFC with 1.0 % and 1.5 % SF, respectively. Finally, the two beams (G1.0SF and G1.5SF), having the same internal reinforcement as beam G0.0SF, were cast using SFC with 1.0 % and 1.5 % SF, respectively. After casting, the beams were left 24 hours in the forms, and then the sides of the forms were stripped away. The beams were cured with water for 28 days. Before testing, a white plastic coat was applied to concrete beams to facilitate observation of cracks during the test.



Figure 4. Beam reinforcement details

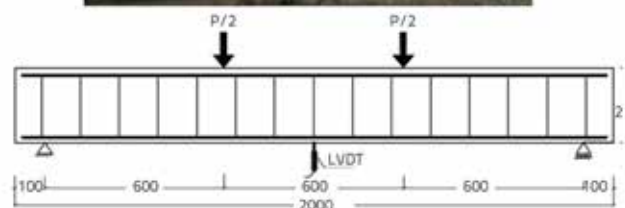


Figure 5. Test setup and instrumentation (dimensions in mm)

The deflection of the beams was measured at midspan using Linear Variable Distance Transducers (LVDTs), having a maximum range of 100 mm. A strain gauge 20 mm in length, with the resistance of $120 \pm 0.3 \Omega$, was glued to the top surface of concrete to quantify compressive strain of concrete. Tensile strain of steel or GFRP bars was measured by a glued strain gauge 5 mm in length, with the resistance of $120 \pm 0.3 \Omega$ in the middle of the bar. A load cell was placed under the hydraulic jack of the testing machine to record the load. Throughout the testing, a data acquisition system was used to record the applied loads, vertical deflection at beam midspan, steel strain, GFRP strain, and concrete strain (see Figure 5).

3. Experimental results

3.1. Effect of SF on concrete properties

Concrete properties determined during experimental tests are presented in Table 4. This table shows that the steel fibre has obvious effect on mechanical properties of concrete, especially with regard to tensile strength, i.e. compressive strength and tensile strength increased gradually when SF ratio is increased up to 1.5%. This observation is also in agreement with the results recorded in [47-51]. The SF acts as a bridge over the crack, and transfers stresses from one side of the crack to another. Also, it helps concrete to assume greater tensile stresses, as it closes the cracks.

Table 4. Concrete results for compressive and tensile strength

Concrete type	SF ratio [%]	Compressive strength [MPa]	Tensile strength [MPa]
NC	0 %	38.7	4.5
FC1	1 %	40.8	5.1
FC2	1.5 %	42.1	5.3

3.2. Load capacity and failure modes

Values obtained during experimental tests are shown in Table 5. The load at initial cracking (P_{cr}), yield load (P_y), maximum load

capacity (P_u), deflection at initial cracking (Δ_{cr}), deflection at yield load (Δ_y), maximum deflection (Δ_u), deformability factor (μ_d), initial stiffness (K_i), ductility appraisal index (μ_E), and failure modes for tested beams, are listed in Table 5. The initial stiffness (K_i) is indicated as the initial slope of the load-deflection curve, and is defined as the ratio of cracking load (P_{cr}) to cracking deflection (Δ_{cr}) [52] as shown in Figure 6. The deformability factor (μ_d) for RC structures with steel was simply defined as the ratio of ultimate deflection (Δ_u) or the deflection corresponding to 85 - 90 % of the maximum recorded load capacity [53] to the yielding deflection (Δ_y).

In this study, the deformability factor (μ_d) for RC beams with steel was calculated as the ratio of the deflection at 85 - 90 % of the maximum recorded load capacity to the yielding deflection (Δ_y) (i.e. $\mu_d = (\Delta_{at\ 0.85\ P_u} / \Delta_y)$).

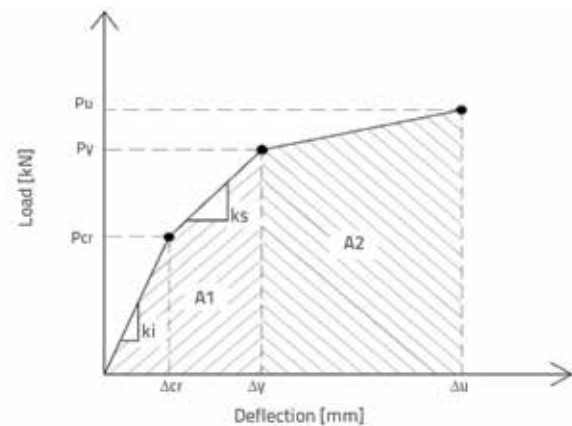


Figure 6. Load-deflection curve with initial stiffness [52]

Due to the linear stress-strain relationship of FRP bars, this traditional definition cannot be applied to FRP reinforced structures. A new model about the deformability factor of FRP reinforced structures was established by Fadi and El-Hacha [54]. The value of deformability factor of a FRP reinforced concrete flexural member can be taken from the deflection corresponding to 75 - 80 % of ultimate loading from the load-deflection curves (i.e. $\mu_d = (\Delta_u / \Delta_{at\ 0.75\ P_u})$). The ductility appraisal index (μ_E) can be defined as the ratio between the total and elastic energy. For FRP reinforced beams, the total energy (E_{tot}) can be determined by

Table 5. Experimental results for tested beams

Beam No	P_{cr} [kN]	P_y [kN]	P_u [kN]	$P_u/P_{u,CB}$ (%)	Δ_{cr} [mm]	Δ_y [mm]	Δ_u [mm]	$\Delta_u / \Delta_{u,CB}$	K_i	μ_E	μ_d	Failure mode
S0.0SF (CB)	20	75	94	-	3	25	55	1	6.66	1.25	1.1	Y, CC
G0.0SF	14	-	96	102	4	-	57	0.9	3.5	1.48	1.18	T, CC
S1.0SF	30	79	104	110	4	21	84	1.52	7.5	1.49	1.24	Y, CC
G1.0SF	22	-	113	120	5	-	80	1.45	4.4	2.2	1.41	T, CC
S1.5SF	35	82	110	117	4	17	85	1.54	8.75	2.08	1.88	Y, CC
G1.5SF	24	-	114	121	5	-	86	1.56	4.8	3.53	2.15	T, CC

Y - steel yielding (reinforcement bars reached yield, i.e. ductile failure), CC - concrete crushing (brittle failure), T - tension failure of GFRP bars

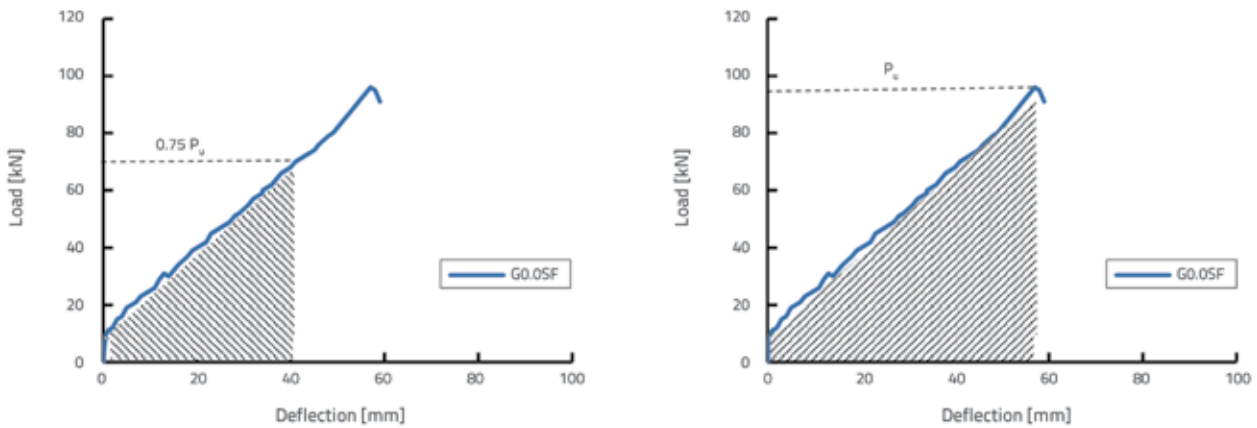


Figure 7. Calculation of ductility appraisal index for specimen G0.05F [55]: a) calculation E_{el} ; b) calculation E_{tot}

the total area under the load-deflection curve up to the failure load, while the elastic energy (E_{el}) can be estimated from the load - deflection curve as 75 % of ultimate load ($E_{0.75u}$) [55] (see Figure 7). For steel reinforced beams, the total energy (E_{tot}) can be determined by the total area under the load-deflection curve up to $0.85 f_y$ and the elastic energy (E_{el}) can be calculated up to yield. The ductility appraisal index (μ_E) can be expressed as:

$$\mu_E = \frac{E_{tot}}{E_{el}} \quad \text{- for beams reinforced with steel bars} \quad (2)$$

$$\mu_E = \frac{E_{tot}}{E_{0.75u}} \quad \text{- for beams reinforced with GFRP bars} \quad (3)$$

Failure modes of tested beams can be divided into two categories. The first category involves ductile flexural failure and the second one brittle compression failure (concrete crushing, CC). No cracks were observed in the un-cracked stage (1st stage). In the post cracking to tension steel pre-yield stage (2nd stage), first micro cracks were observed for beams reinforced with steel and GFRP bars. The first crack was initiated at the bottom of the beam between two loading points (pure bending). As the load progressed, more cracks started to appear and propagate toward the top of the beam, but crack widening could not be observed by visual inspection. The third stage for beams reinforced with steel bars started from tension steel post yield stage and ended with failure. In this stage, the cracks became wider and longer than before when the beam failed due to compression failure (concrete crushing), as shown in Figure 8a. The beam G0.05F, reinforced in tension with GFRP bars, failed due to

one of the GFRP bars rupture, which was followed by concrete crushing (Figure 8b). The failure of SFC beams reinforced in tension with steel or GFRP bars was flexural failure, followed by concrete crushing (see Figures 8c to 8e). The flexural failure started with cracks that formed at the midspan of the beam. As loading progressed, more cracks were formed, and steel fibres bridging was also observed. Afterwards, the start of steel fibres pull out from concrete matrix was observed. The fibres were pulled out at the sections where the beams reached their ultimate load capacities. The width of the cracks became clear and wider compared to other cracks in the beam. Generally, the cracks in beams reinforced with steel bars were narrower than those in beams reinforced with GFRP bars (Figure 8) as GFRP bars have lower stiffness than steel ones.

The portion of steel bars located inside the midspan of the crack experienced high elongation, after which the load application



Figure 8. Crack patterns and modes of failure: a) S0.05F (CB); b) G0.05F; c) S1.05F; d) S1.55F; e) G1.55F

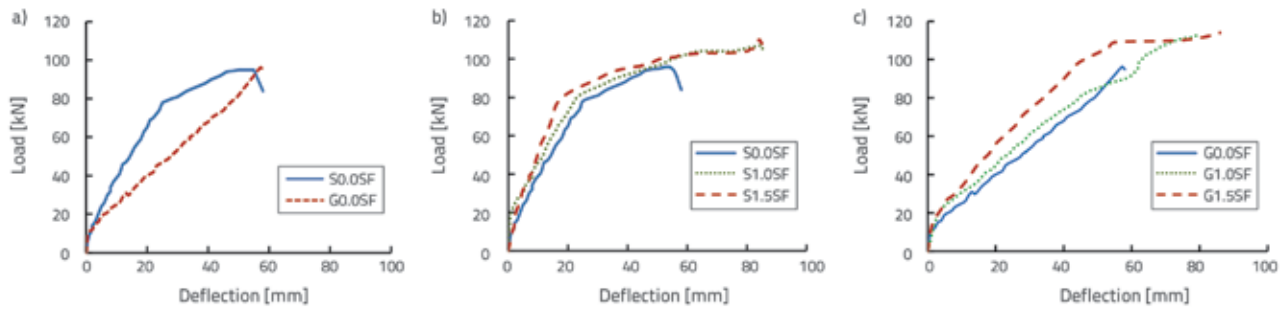


Figure 9. Load-deflection for all tested beams: a) Influence of type of reinforcement; b) Effect of steel fiber content in case of steel reinforcement; c) Effect of steel fiber content in case of GFRP reinforcement

was stopped. The load capacity of NC beams reinforced with GFRP was nearly the same as the load capacity of beams reinforced with steel (the difference being 2 % only, Table 4). By increasing the percentage of SF, the load carrying capacity of RC beams also increased. For RC beams with steel reinforcement, the load capacity increased by 10 % and 17 % by adding 1 % and 1.5 % of SF, respectively. On the other hand, by adding 1 % and 1.5 % SF to RC beams reinforced with GFRP bars their load capacities increased by 20 % and 21 %, respectively. These findings prove that flexural behaviour (maximum load, deformability, and ductility) or RC beams improves if SF is added. Similar findings were also reported in [56], where it is indicated that, by adding 1 % of hooked SF to RC beams with FRP, their ductility improved, and was similar to that of RC beams with steel bars.

3.3 Load - deflection response

Figure 9 shows the midspan load to deflection ratio for the tested RC beams. All tested beams passed through three stages of response up to failure. In the un-cracked stage (1st stage), the load was increased linearly. In the 2nd stage, a linear relation was also observed for all tested beams, with an increase in beam deflection. In the third stage, for beams reinforced with steel bars, the stiffness of the beams decreased with an increase in beam deflection. In contrast, the third stage was not clear for beams reinforced with GFRP bars due to linear elastic behaviour of FRP materials. The stiffness of load deflection curves for RC beams with GFRP bars was influenced by SF pullout only. It was clear that SF in concrete allowed RC beams to experience

more deflection before failure in addition increasing their load capacity, initial stiffness, and deformation capacity. The increase in stiffness of the RC beams due to SF effect is in accordance with similar findings reported in [57]. Also, when using GFRP bars instead of steel ones, the cracking load was reduced. Convergence in the value of ultimate load between the two cases was also noted.

The results have shown that the change in beam tension reinforcement from steel to GFRP for beams cast with NC results in a decrease of initial stiffness by about 47.4 % for RC beams without steel fibre. This is due to the fact that GFRP bars have a low elastic modulus, which prompted the sudden loss in the RC beam stiffness. In addition, the use of GFRP instead of steel as internal reinforcement increased the ductility appraisal index by about 18.4 % for RC beams without SF. On the other hand, the initial stiffness, ductility appraisal index, and deformability ratio, increased when the RC beams with steel or GFRP bars were cast with SFC.

3.4. Compressive strain

Compressive strain was measured on top surface of the tested beams. Test results showed that the compressive strain of concrete was directly proportional to the amount of steel fibres. Also, in the case of the tested beams cast with NC, once the ultimate load was attained, the failure occurred by concrete crushing, and reinforcement strain dropped suddenly. In contrast, in the case of beams cast with FC, the reinforcement strain kept increasing until failure. Figure 10

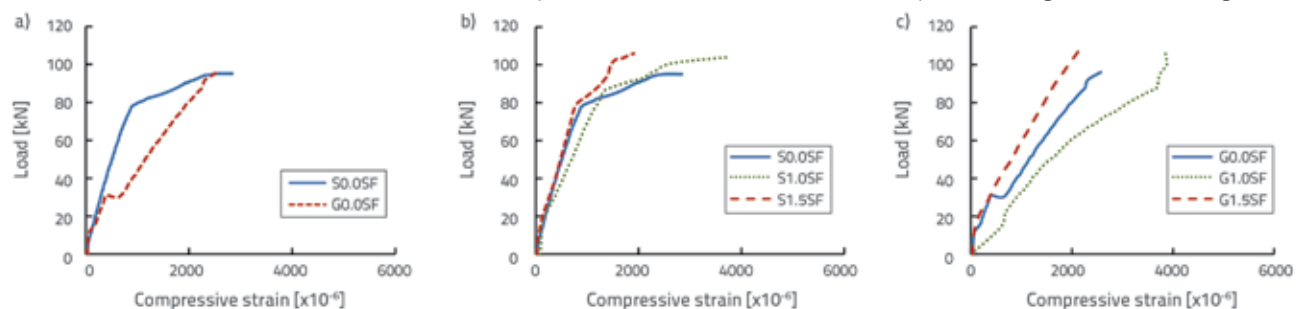


Figure 10. Load - compressive strain for all tested beams: a) the influence of the type of reinforcement; b) the effect of the proportion of steel fibers in the case of steel reinforcement; c) effect of steel fiber content in case of GFRP reinforcement

shows load - compression strain curves for all beams subjected to testing. This figure demonstrates that the use of GFRP bars instead of steel bars resulted in an increase in compressive strain for beams cast without SF (NC). For beams reinforced with steel bars and cast with FC (1 % SF), the compressive strain increased insignificantly despite the fact that 1.5 % of SF reduced the compressive strain by a very small amount. A more noticeable result was obtained in the case of RC beams with GFRP bars.

4. Numerical analysis

In this study, a numerical analysis was carried out using ANSYS 15 F.E program to study the behaviour of RC beams having different internal reinforcement and cast with NC and SFC. Work diagrams for materials, uniaxial elastic modulus, tensile strength, and Poisson's ratio for concrete, were defined as related to experimental outputs, the aim being to create a model with and without steel fibres in ANSYS. Extensive numerical trials and matching experimental data were used to adopt the values of Poisson's ratio for NC and SFC [58]. The concrete smeared cracking was included in all models to simulate the response of NC and SFC. Multilinear isotropy for concrete is represented by points in the stress-strain curve. The strain of concrete at ultimate stress is almost constant and equal to 0.2 %, while the failure strain is approximately equal to 0.3 % as noted in ECP 203-2007 [59]. and, in the case of high-strength concrete, it approaches 0.004 as noted in ACI and CSA codes. The ascending part of the curve is taken to be a parabola as defined by Hognestad's [60], and the remaining part of the curve is assumed to be constant (idealized curve) (see Figure 11a). The stress - strain relationship can be defined according to the following Eq. (4):

$$f_c = 0.67f_{cu} \left[\frac{2\varepsilon_c}{\varepsilon_0} - \left(\frac{\varepsilon_c}{\varepsilon_0} \right)^2 \right] \tag{4}$$

where:

- E_c - the concrete elasticity modulus
- f_c - the concrete stress at a certain strain
- f_{cu} - the concrete compressive strength
- ε_c - the concrete strain, $\varepsilon_0 = 0.002$.

The ultimate compressive stress of concrete in compression equals to $(0.67 f_{cu})$ as noted in ECP 203-2007 [59]. To remove the cracking and crushing capability, a value of -1 for constant

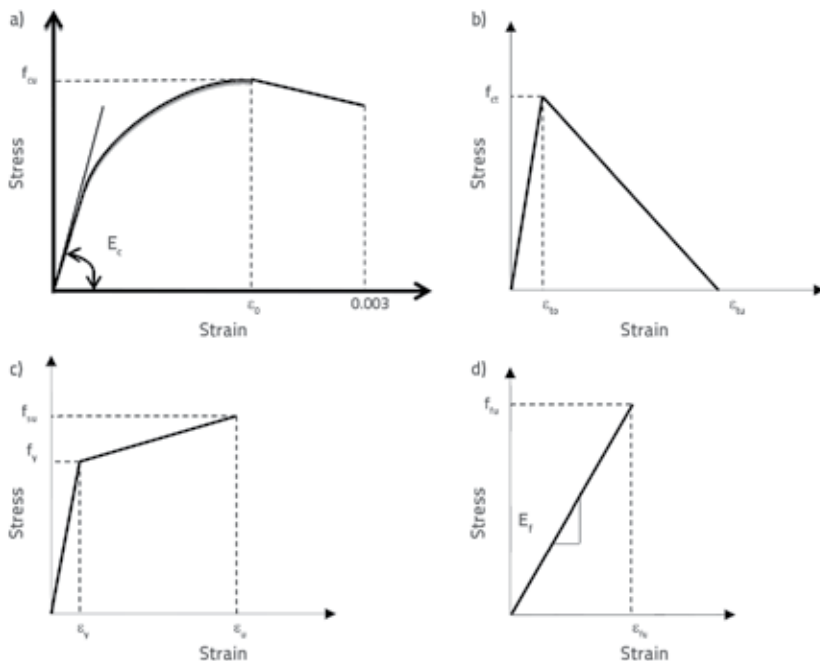


Figure 11. Stress - strain curves used to model concrete, steel and GFRP bars: a) Concrete in compression; b) Concrete in tension; c) Steel; d) FRP

uniaxial cracking stress or uniaxial crushing stress also removes the cracking or crushing capability, respectively. Also, stress strain-curves used to model concrete in tension are shown in Figure 11b (f_{tu} is the concrete tensile strength, ε_{to} and ε_{tu} are the strain at f_{tu} and at failure, respectively). To model RC beams in ANSYS, an element (Solid 65) was used for concrete with or without SF. Solid 65 element has eight nodes with six degrees of freedom at each node (3 displacements and 3 rotations). This element is shaped as rectangular prism and it has a plastic deformation capability, with cracking in three orthogonal directions. A schematic of Solid 65 element is shown in Figure 12.

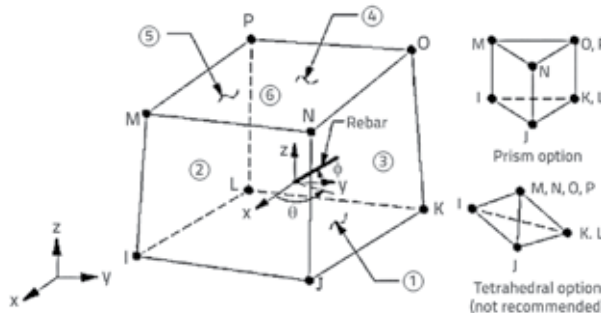


Figure 12. Solid 65 element (ANSYS)

The real constant was adopted for the element (Solid 65) to include the volume fraction of SF in concrete. The chosen parameter for the concrete with and without SF, determined via sensitivity analysis, is reported in Table 6.

Table 6. Parameters adopted for three types of concrete

Parameter	NC (without SF)	FC (1 % SF)	FC (1.5 % SF)
Poisson's ratio, ν	0.2	0.225	0.225
Uniaxial crushing stress [MPa]	36	38	39
Uniaxial cracking stress [MPa]	3.6	4.5	5
Open shear transfer coefficient	0.2	0.5	0.5
Closed shear transfer coefficient	0.8	0.8	0.8

$E_c = 440 \times [59]$ where E_c is the modulus of elasticity for concrete and f_{cu} is the compressive strength of concrete at 28 days.

In the present study, the beam was modelled using discrete reinforcement. Therefore, a value of zero was entered for real constants, which turned off the smeared reinforcement capability of the Solid 65 element.

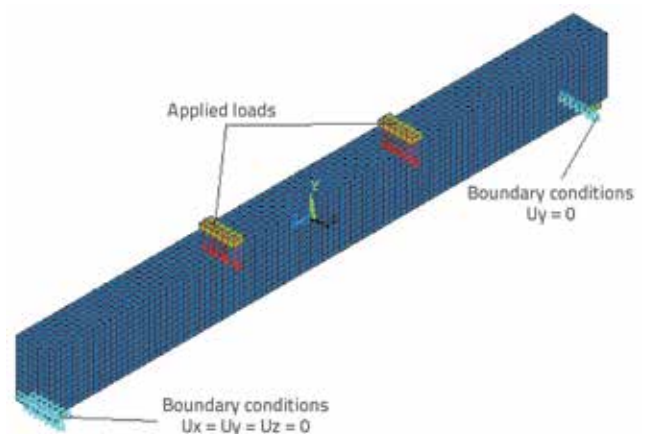
Tensile plasticity was implemented to represent behaviour of steel bars, while FRP bars were simulated as being elastic up to failure (Figs. 11c and 11d, respectively). where f_{sd} , f_y , ϵ_y and ϵ_d are the tensile strength, yield strength, yield strain, and ultimate strain of steel, respectively, while E_p , f_{tu} and ϵ_{tu} are the elasticity modulus, ultimate strength, and strain of FRP, respectively. Detailed parameters for GFRP bars were adopted in accordance with experimental values. Properties of AFRP and CFRP bar materials were taken from the Egyptian code of Practice (ECP 208-2005 [61]), i.e. the modulus of elasticity was 70 GPa and 110 GPa, respectively. An appropriate element (Solid 185) was chosen for the steel loading plates. It is an eight-node element with three degrees of freedom. An element (Link 180) was included to represent the steel, FRP and stirrups reinforcement. It is a 3D element with three degrees of freedom. The real constant for Link 180 represents the cross-sectional area for steel elements, FRP bars, and stirrups. The perfect bond between concrete and internal reinforcement was assumed. Rebars were connected to the corresponding concrete elements to avoid slip between the internal reinforcement and concrete. Figure 13 shows the ANSYS model that represents the loads, supports, and boundary conditions.

All meshes of concrete elements were symmetric cubes, which distorted each time after tensile or compressive failure. The beam section was discretised due to transverse and longitudinal symmetry. The standard Newton-Raphson method was used to solve the nonlinear equilibrium equation using the finite element method in ANSYS, which was presented by engineer Vladimir Ivanko [62]. The mesh size of 25 mm was adopted for all modelled beams in accordance with the conducted sensitivity analysis. Convergence criteria of the finite element method were defined as related to displacement with the tolerance

of 0.01. This tolerance can be increased to reduce the time increment and the number of the sub steps that are needed to reach perfect solution for the studied beams.

4.1. Verification of FEM

Experimental results were used to verify the modelled beams. Figure 14 shows load - deflection curves for experimental (E) and finite (F) element models. The figure shows a good agreement between numerical and experimental results. This agreement confirmed that the model was capable of simulating, with considerable accuracy, the concrete beams internally reinforced with FRP or steel reinforcement.

**Figure 13. Finite element mesh and boundary conditions of the Model**

4.2. Parametric study and numerical results of simulated beams

A parametric study was performed using the verified model. The effect of FRP bars type (glass, aramid, and carbon), reinforcement ratio (0.54 % and 0.913 %), and SF volume fraction (0 %, 1 %, and 1.5 %) on flexural behaviour of beams was studied in this numerical parametric study. The parametric study was performed in two groups (Group A and Group B). The first group (A) consists of concrete beams internally reinforced with the reinforcement ratio of (ρ_s) = 0.54 % (3 bars 16 mm in diameter). The second group (B) consists of concrete beams reinforced internally with the reinforcement ratio of (ρ_s) = 0.913 % (5 bars 16 mm in diameter). The modelled beams were subjected to displacement control loading up to failure.

Table 7 shows numerical results of the simulated beams in terms of cracking load (P_c), yield load (P_y) and ultimate load (P_u). This table shows that ultimate load values of simulated beams increases with an increase in SF and internal reinforcement ratios.

On the other hand, the ultimate loads of the beams with GFRP bars and steel reinforcement were close to each other while the beams reinforced with AFRP and CFRP bars displayed higher

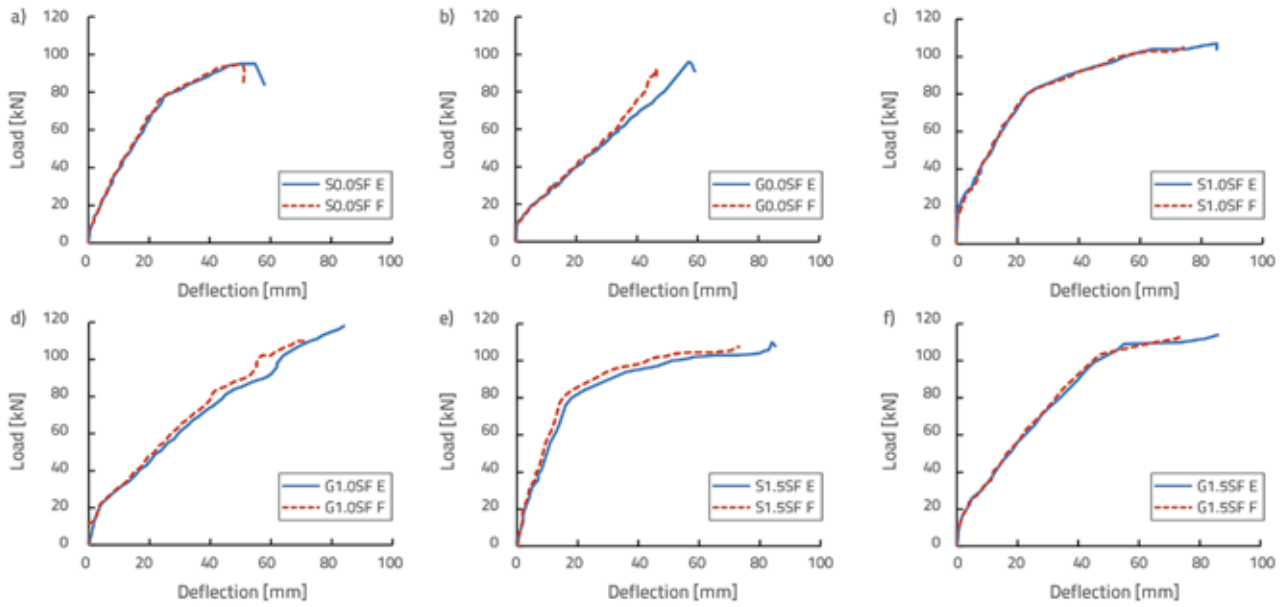


Figure 14. Comparison between experimental and numerical results: a) steel bars with 0 % SF; b) GFRP bars with 0 % SF; c) steel bars with 1.0 % SF; d) GFRP bars with 1.0 % SF; e) steel bars with 1.5 % SF; f) GFRP bars with 1.5 % SF

Table 7. Numerical results for simulated beams

Specimen, ID	V_f [%]	Type of bars	No. of bars	P_{cr} [kN]	P_v [kN]	P_u [kN]
3S0SF	0	Steel	3	30	125	139
3G0SF		Glass	3	13	-	135
3A0SF		Aramid	3	20	-	161
3C0SF		Carbon	3	29	-	206
5S0SF	0	Steel	5	44	187	202
5G0SF		Glass	5	24	-	166
5A0SF		Aramid	5	30	-	220
5C0SF		Carbon	5	37.5	-	278
3S1SF	1	Steel	3	37	131	149
3G1SF		Glass	3	16	-	141
3A1SF		Aramid	3	25	-	164
3C1SF		Carbon	3	30	-	210
3S1.5SF	1.5	Steel	3	41	139	155
3G1.5SF		Glass	3	17.5	-	144
3A1.5SF		Aramid	3	28.7	-	169
3C1.5SF		Carbon	3	33	-	216
5S1SF	1	Steel	5	50	192	207
5G1SF		Glass	5	26	-	171
5A1SF		Aramid	5	33	-	228
5C1SF		Carbon	5	44	-	283
5S1.5SF	1.5	Steel	5	55	205	215
5G1.5SF		Glass	5	26	-	188
5A1.5SF		Aramid	5	36	-	239
5C1.5SF		Carbon	5	46	-	288

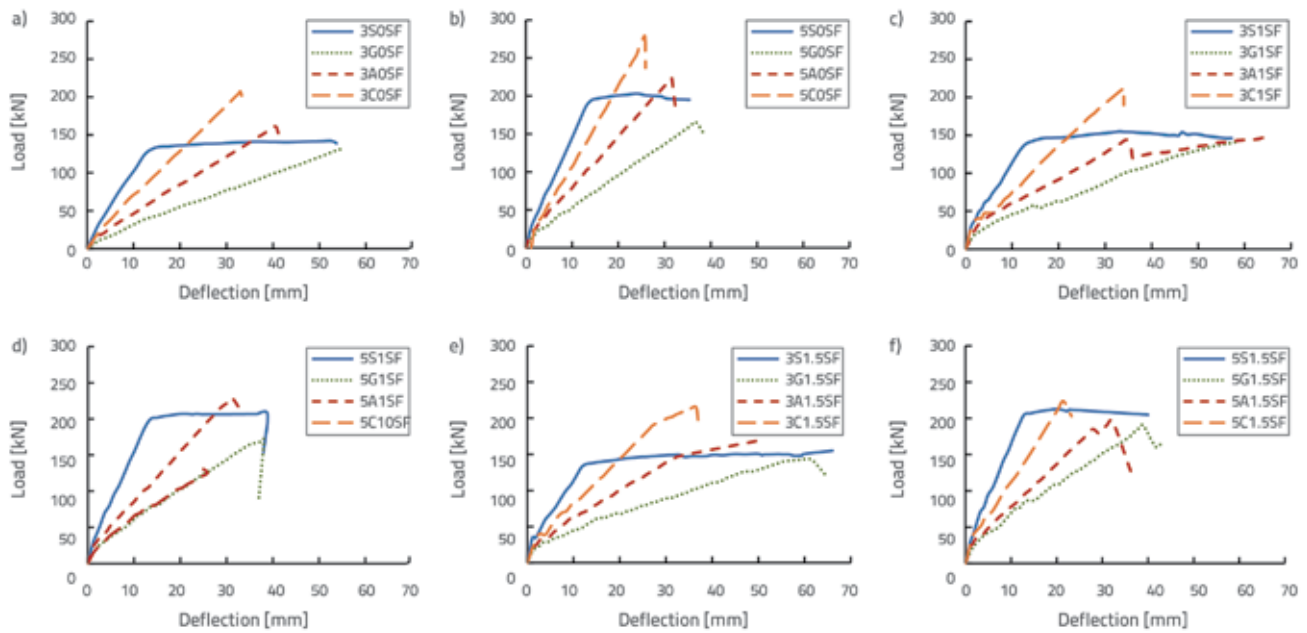


Figure 15. Load-deflection for all studied beams: a) 0 % SF and ρ_1 ; b) 0 % SF and ρ_2 ; c) 1.0 % SF and ρ_1 ; d) 1.0 % SF and ρ_2 ; e) 1.5 % SF and ρ_1 ; f) 1.5 % SF and ρ_2

load bearing capacities. Also, ultimate loads of concrete beams were slightly higher in case the SF was used, regardless of the internal reinforcement ratio (ρ_1 and ρ_2).

The ultimate load of beams reinforced with AFRP and CFRP increased by 15 % and 48 %, respectively, compared to control beams reinforced with steel bars, when the internal reinforcement ratio was (ρ_1) = 0.54 %. On the other hand, the ultimate load of the beams reinforced by AFRP and CFRP increased by 9 % and 37 %, respectively, compared to control beams reinforced by steel bars, when the internal reinforcement ratio was (ρ_2) = 0.913 %. Moreover, an increase in ρ value from 0.54 % to 0.913 % increased the ultimate load of the simulated beams reinforced with steel, GFRP, AFRP and CFRP bars by 45 %, 23 %, 36.6 %, and 35 %, respectively.

Finally, it can be noticed that an increase in volume fraction of SF from 0 % to 1.5 % leads to small increase in the ultimate load of simulated beams. For beams with ρ_1 internal reinforcement, the ultimate load of the beams reinforced with steel, GFRP, AFRP, and CFRP bars increased by 11.5 %, 6.6 %, 5 %, and 4.8 %, respectively, when the SF increased from 0 to 1.5 %. On the other hand, for beams with ρ_2 internal reinforcement, the ultimate load of the beams reinforced with steel, GFRP, AFRP, and CFRP bars increased by 6.4 %, 13 %, 5 % and 8.6 %, respectively, when the SF increased from 0 to 1.5 %.

Load-deflection curves were plotted to represent the relation between the load and central deflection for beams simulated at various stages of loading, as shown in Figure 15. All simulated beams exhibited linear behaviour from initial loading up to the first crack. After the 1st crack, FRP reinforced beams continued to exhibit semi-linear behaviour until failure. The beams with SF tended to be stiffer than those without SF. The deformability factor (μ_f) and the ductility appraisal index

(μ_d), were calculated for all simulated beams, using the above mentioned definition.

An increase in ρ ratio from 0.54 % to 0.913 % for simulated beams caused a decrease in the beam deformability factor. In the case of 0 % SF, the deformability factor decreased by 13.6 %, 2.9 %, 2.8 %, and 0.8 % for steel, GFRP, AFRP, and CFRP bars, respectively. In the case of 1.5 % steel fibres, the deformability factor decreased by 12.1 %, 9.8 %, 8.3 %, and 1.2 % for steel, GFRP, AFRP, and CFRP bars, respectively.

In contrast, the deformability factor of simulated beams augmented in case the SF ratio was increased from 0 % to 1.5 %. For beams with ρ_1 , an increase in SF ratio from 0 to 1 % augmented the deformability factor by 7.2 %, 8 %, 21.4 %, and 9.2 % for steel, GFRP, AFRP and CFRP bars, respectively. Moreover, by increasing the SF ratio from 0 % to 1.5 %, the deformability factor increased by 12.8 %, 27 %, 29.3 % and 26.9 % for steel, GFRP, AFRP and CFRP bars, respectively.

For beams with ρ_2 an increase in the SF ratio from 0 % to 1 % augmented the deformability factor by 7.4 %, 12 %, 14 %, and 11.6 % for steel, GFRP, AFRP, and CFRP bars, respectively, while the deformability factor increased by 14.8 %, 18 %, 22 %, and 26.4 % for steel, GFRP, AFRP, and CFRP bars respectively when SF ratio changed from 0 to 1.5 %.

The type of internal reinforcement greatly affected the ductility appraisal index (μ_E) of simulated beams. The change of internal reinforcement type with ρ_1 ratio from steel to GFRP, AFRP and CFRP bars increased μ_E by 23.7 %, 22.4 % and 14.5 %, respectively. The change of internal reinforcement type with ρ_2 ratio from steel to GFRP, AFRP and CFRP bars increased μ_E by 50 %, 52.5 % and 45.8 %, respectively.

Moreover, an increase in SF % from 0 % to 1.5 % increased μ_E of simulated beams. For beams with internal reinforcement

ratio ρ_1 , the values of μ_E increased by 13.2 % and 21.1 % (steel), 9.8 % and 28.8 % (GFRP), 28 % and 42.5 % (AFRP) and 18.4 % and 31.6 % (CFRP) when the SF changed from 0 % to 1 and from 0 % to 1.5 %, respectively. On the other hand, for beams with internal reinforcement ratio ρ_2 , the values of μ_E increased by 11.9 % and 25.4 % (steel), 5.6 % and 22.6 % (GFRP), 15.8 % and 28.3 % (AFRP), and by 13.4 % and 32 % (CFRP) when the SF changed from 0 % to 1 % and from 0 % to 1.5 %, respectively. Finally, an increase in the internal reinforcement ratio (ρ) from 0.54 % to 0.913 % for simulated beams decreased the values of μ_E . In the case of 0 % SF, the values of μ_E decreased by 22.4 %, 5.9 %, 3.2 % and 1.15 % for steel, GFRP, AFRP, and CFRP bars, respectively.

5. Conclusions

In this study, experimental and numerical works were conducted to study the effect of using (FRP) bars and SF on flexural response of RC beams. Based on the results obtained in this study, the following conclusions can be made:

- The load capacity of tested RC beams with steel and GFRP bars increased with an increase in SF %. For RC beams with steel reinforcement, the load capacity increased by 10 % and 17 % after adding 1 % and 1.5 % of SF, respectively. On the other hand, after adding 1 % and 1.5 % of SF to RC beams reinforced with GFRP bars, their load capacities increased by 20 % and 21 %, respectively.
- The use of GFRP instead of steel as internal reinforcement increased the ductility appraisal index by about 18.4 % for RC beams without SF, while the initial stiffness decreased by about 47.4 %.
- It was established by numerical analysis that the ultimate load of the beams reinforced by AFRP and CFRP increased by 15 % and 48 %, respectively, compared by the control beams reinforced with steel bars, when the internal reinforcement ratio amounted to (ρ_1) = 0.54 %. On the other hand, the ultimate load of the beams reinforced with AFRP and CFRP increased by 9 % and 37 %, respectively, compared to control beams reinforced by steel bars, when the internal reinforcement ratio amounted to (ρ_2) = 0.913 %.
- An increase of ρ ratio from 0.54 % to 0.913 % for simulated beams caused a decrease in the beam deformability factor. In the case of 0 % of SF, the deformability factor decreased by 13.6 %, 2.9 %, 2.8 %, and 0.8 % for steel, GFRP, AFRP and CFRP bars, respectively. In the case of 1.5 % of steel fibres, the deformability factor decreased by 12.1 %, 9.8 %, 8.3 %, 1.2 % for steel, GFRP, AFRP, and CFRP bars, respectively.
- The type of internal reinforcement greatly affected the ductility appraisal index (μ_E) of simulated beams. The change of internal reinforcement type with ρ_1 ratio from steel to GFRP, AFRP and CFRP bars increased μ_E by 23.7 %, 22.4 %, and 14.5 % respectively. The change of internal reinforcement type with ρ_2 ratio from steel to GFRP, AFRP and CFRP FRP bars increased μ_E by 50 %, 52.5 %, and 45.8 %, respectively.

REFERENCES

- [1] El-Salakawy, E.F., Benmokrane, B.: Serviceability of concrete bridge deck slabs reinforced with FRP composite bars, *ACI Structural Journal*, 101 (2014) 5, pp. 727–36
- [2] Rashid, M., Mansur, M., Paramasivam, P.: Behavior of aramid fiber-reinforced polymer reinforced high strength concrete beams under bending, *Journal of Composites for Construction*, 9 (2005) 2, pp. 117–27
- [3] Duic, J., Kenno, S., Das, S.: Performance of concrete beams reinforced with basalt fibre composite rebar, *Construction and Building Materials*, 176 (2018) 10, pp. 470–81
- [4] Rafi, M.M., Nadjai, A., Ali, F., Talamona, D.: Aspects of behaviour of CFRP reinforced concrete beams in bending, *Construction and Building Materials*, 22 (2018) 3, pp. 277–85
- [5] El-Nemr, A., Ahmed, E.A., Benmokrane, B.: Flexural behavior and serviceability of normal-and high-strength concrete beams reinforced with glass fiber-reinforced polymer bars, *ACI Structural Journal*, 110 (2013) 6, pp. 1077
- [6] El-Nemr, A., Ahmed, E.A., Barris, C., Benmokrane, B.: Bond-dependent coefficient of glass-and carbon-FRP bars in normal-and high-strength concretes, *Construction and Building Materials*, 113 (2016) 15, pp. 77–89
- [7] Rahman, S.H., Mahmoud, K., El-Salakawy, E.: Behavior of glass fiber-reinforced polymer reinforced concrete continuous T-beams, *Journal of Composites for Construction*, 21 (2016) 2, 04016085
- [8] Al-Sunna, R., Pilakoutas, K., Hajirasouliha, I., Guadagnini, M.: Deflection behaviour of FRP reinforced concrete beams and slabs: An experimental investigation, *Composites Part B: Engineering*, 43 (2012) 5, pp. 2125–3214
- [9] Yang, J.M., Min, K.H., Shin, H.O., Yoon, Y.S.: Effect of steel and synthetic fibers on flexural behavior of high-strength concrete beams reinforced with FRP bars, *Composites Part B: Engineering*, 43 (2012) 3, pp. 1077–1086
- [10] Yoo, D.Y., Banthia, N., Yoon, Y.S.: Flexural behavior of ultra-high-performance fiber reinforced concrete beams reinforced with GFRP and steel rebars, *Engineering Structures*, 111 (2016) 15, pp. 246–262
- [11] Vijay, P.V., GangaRao, H.V.: Bending behavior and deformability of glass fiber-reinforced polymer reinforced concrete members, *Journal of Structural Engineering*, 98 (2001) 6, pp. 834–842
- [12] Wang, H., Belarbi, A.: Ductility characteristics of fiber-reinforced-concrete beams reinforced with FRP rebars, *Construction and Building Materials*, 25 (2011) 5, pp. 2391–2401
- [13] Mohamed, N., Farghaly, A.S., Benmokrane, B.: Aspects of deformability of concrete shear walls reinforced with glass fiber-reinforced bars, *Journal of Structural Engineering*, 19 (2014) 5, 06014001
- [14] Oehlers, D.J., Seracino, R.: Design of FRP and steel plated RC structures: retrofitting beams and slabs for strength, stiffness and ductility, Elsevier, Oxford, United Kingdom, 2004.

- [15] Bank, L.C.: Composites for construction: structural design with FRP materials, John Wiley & Sons, New York, 2006.
- [16] Holloway, L.C., Teng, J.G.: Strengthening and rehabilitation of civil infrastructures using fibre-reinforced polymer (FRP) composites, Woodhead Publishing Limited, Cambridge, UK, 2008.
- [17] Jakubovskis, R., Kaklauskas, G., Gribniak, V., Weber, A., Juknys, M.: Serviceability analysis of concrete beams with different arrangements of GFRP bars in the tensile zone, *Journal of Composites for Construction*, 18 (2014) 5, 04014005
- [18] Safan, M.A.: Flexural behavior and design of steel-GFRP reinforced concrete beams, *ACI Materials Journal*, 110 (2013) 6, pp. 677
- [19] Adam, M.A., Said, M., Mahmoud, A.A., Shanour, A.S.: Analytical and experimental flexural behavior of concrete beams reinforced with glass fiber reinforced polymers bars, *Construction and Building Materials*, 84 (2015), pp. 354–366
- [20] Islam, S., Afefy, H.M., Sennah, K., Azimi, H.: Bond characteristics of straight and headed-end, ribbed-surface, GFRP bars embedded in high-strength concrete, *Construction and Building Materials*, 83 (2015), pp. 283–98
- [21] Omar, I., Abdelkarim, E., Ahmedb, A., Hamdy, M.M., Benmokrane, B.: Flexural strength and serviceability evaluation of concrete beams reinforced with deformed GFRP bars, *Engineering Structures*, 186 (2019), pp. 282–296
- [22] Maranan, G.B., Manalo, A.C., Benmokrane, B., Karunasena, W., Mendis, P., Nguyen, T.Q.: Flexural behavior of geopolymer-concrete beams longitudinally reinforced with GFRP and steel hybrid reinforcements, *Engineering Structures*, 182 (2019), pp. 141–152
- [23] Yang, W., He, H., Dai, L.: Damage behaviour of concrete beams reinforced with GFRP bars, *Composite Structures*, 161 (2017), pp. 173–186
- [24] Araba, A.M., Ashour, A.F.: Flexural performance of hybrid GFRP-Steel reinforced concrete continuous Beams, *Composites Part B: Engineering*, 154 (2018), pp. 321–336
- [25] Habeeb, M., Ashour, A.F.: Flexural behavior of continuous GFRP reinforced concrete beams, *ASCE Journal of Composites for Construction*, 12 (2008), pp. 115–24
- [26] Mahroug, M., Ashour, A.F., Lam, D.: Experimental response and code modeling of continuous concrete slabs reinforced with BFRP bars, *Composite Structures*, 107 (2014), pp. 664–674
- [27] Mahroug, M., Ashour, A.F., Lam, D.: Tests of continuous concrete slabs reinforced with carbon fibre reinforced polymer bars, *Composites Part B: Engineering*, 66 (2014), pp. 348–357
- [28] Bischoff, P.H., Gross, S.: Design approach for calculating deflection of FRP reinforced concrete, *ASCE Journal of Composites for Construction*, 15 (2011) 4, pp. 490–499
- [29] Bischoff, P.H., Gross, S.: Equivalent moment of inertia based on integration of curvature, *ASCE Journal of Composites for Construction*, 15 (2011) 3, pp. 263–273
- [30] Mousavi, S.R., Esfahani, M.R.: Effective moment of inertia prediction of FRP-reinforced concrete beams based on experimental results, *ASCE Journal of Composites for Construction*, 16 (2012) 5, pp. 490–498
- [31] Correia, J.R., Branco, F.A., Ferreira, J.G.: Flexural behaviour of GFRP-concrete hybrid beams with interconnection slip, *Composite Structures*, 77 (2007), pp. 66–78
- [32] Correia, J.R., Branco, F.A., Ferreira, J.: GFRP-concrete hybrid cross-sections for floors of buildings, *Engineering Structures*, 31 (2009), pp. 1331–1343
- [33] Correia, J.R., Branco, F.A., Ferreira, J.G.: Flexural behaviour of multi-span GFRP concrete hybrid beams, *Engineering Structures*, 31 (2009), pp. 1369–1381
- [34] Santos, N., La Rovere, H.L.: Composite concrete/GFRP slabs for footbridge deck systems, *Composite Structures*, 92 (2010), pp. 2554–2564
- [35] Mendes, P.J.D., Barros, J.A.O., Sena-Cruz, J.M., Taheri, M.: Development of a pedestrian bridge with GFRP profiles and fiber reinforced self-compacting concrete deck, *Composite Structures*, 93 (2011), pp. 2969–2982
- [36] El-Hacha, R., Chen, D.: Behaviour of hybrid FRP-UHPC beams subjected to static flexural loading, *Composites Part B: Engineering*, 43 (2012), pp. 582–593
- [37] Neagoe, C.A., Gil, L., Pérez, M.A.: Experimental study of GFRP-concrete hybrid beams with low degree of shear connection, *Construction Building Materials*, 101 (2015), pp. 141–51
- [38] Nguyen, H., Rahall, N.J., Zatar, W.: Flexural behavior of hybrid composite beams, *Transportation Research Record Journal of the Transportation Research Board*, (2013), pp. 53–63
- [39] Gonilha, J.A., Barros, J., Correia, J.R., Sena-Cruz, J., Branco, F.A., Ramos, L.F. et al.: Static, dynamic and creep behaviour of a full-scale GFRP-SFRSCC hybrid footbridge, *Composite Structures*, 118 (2014), pp. 496–509
- [40] Hulatt, J., Holloway, L., Thorne, A.: The use of advanced polymer composites to form an economic structural unit, *Construction Building Materials*, 17 (2003), pp. 55–68
- [41] Koaik, A., Bel, S., Jurkiewicz, B.: Shear connections between GFRP pultruded profiles and concrete: A comparison between bolting and bonding, *MechComp*, Munich, 2016.
- [42] Zheng, Y., Wu, X., He, G., Shang, O, Xu, J., Sun, Y.: Mechanical properties of steel fiber-reinforced concrete by vibratory mixing technology, *Advances in Civil Engineering*, (2018)
- [43] BS EN 12390-3 :2009: Testing Hardened Concrete, Compressive Strength of Test Specimens
- [44] BS EN 12390-6:2009: Testing hardened concrete, Tensile splitting strength of test specimens
- [45] ASTM A370: Standard test methods and definitions for mechanical testing of steel produces, American Society of Testing and Materials, Pennsylvania, USA, 2010.
- [46] ACI 440.3R-12: Guide for test methods for fiber reinforced polymers (FRP) for reinforcing and strengthening concrete structures, ACI committee 440, American Concrete Institute, Farmington Hills, MI, 2012.
- [47] Tanoli, W.A., Naseer, A., Wahab, F.: Effect of Steel Fibers on Compressive and Tensile Strength of Concrete, *International Journal of Advanced Structures and Geotechnical Engineering*, 3 (2014) 4, pp. 393-397
- [48] Jayswal, S.D., Hansora, A.G., Pandya, A.A.: Effect of Steel Fibres on Compressive & Tensile Strength of Concrete using M -Sand as Fine Aggregate, *International Journal of Engineering Research & Technology*, 4 (2015) 5, pp. 189-194
- [49] Zheng, Y., Wu, Y., He, G., Shang, Q., Xu, J., Sun, Y.: Mechanical Properties of Steel Fiber-Reinforced Concrete by Vibratory Mixing Technology, *Advances in Civil Engineering*, (2018).
- [50] Abbass, W., Khan, M.I., Mourad, S.: Evaluation of mechanical properties of steel fiber reinforced concrete with different strengths of concrete, *Construction and Building Materials*, 168 (2018), pp. 556–569

- [51] Wang, X., Zhang, S., Wang, C., Cao, K., Wei, P., Wang, J.: Effect of steel fibers on the compressive and splitting-tensile behaviors of cellular concrete with millimeter-size pores, *Construction and Building Materials*, 221 (2019), pp. 60–73
- [52] Sullivan, T.J., Calvi, G.M., Priestley, M.J.: Initial stiffness versus secant stiffness in displacement-based design, *Proceedings of the 13th World Conference on Earthquake Engineering*, Vancouver, B.C., Canada 2004, pp. 1-16
- [53] Ahmed, M., Farghal, O., Nagah, A., Haridy, A.: Effect of Confining Method on the Ductility of over-Reinforced Concrete Beams, *Journal of Engineering Sciences*, 35 (2007) 3, pp. 617-633
- [54] Fadi, O., El-Hacha, R.A.: New Ductility Model of Reinforced Concrete Beams Strengthened Using Fiber Reinforced Polymer Reinforcement, *Composites Part B: Engineering*, 43 (2012) 8, pp. 3338-3347
- [55] Spadea, G., Bencardino, F., Swamy, R.N.: Strengthening and Upgrading Structures with Bonded CFRP Sheets, *Design Aspects for Structural Integrity, Proceedings of the 3rd International RILEM Non-Metallic (FRP) for Concrete Structures*, Sapporo, Japan, 1997, pp. 379-386
- [56] Alsayed, S.H., Alhozaimy, A.M.: Ductility of Concrete Beams Reinforced with FRP Bars and Steel Fibers, *Journal of Composite Materials*, 33 (1999) 19, pp. 1792-1806, doi:10.1177/002199839903301902
- [57] Ranjbaran, F., Rezayfar, O., Mirzababai, R.: Experimental investigation of steel fiber reinforced concrete beams under cyclic loading, *International Journal of Advanced Structural Engineering*, (2018) 10, pp. 49–60
- [58] Islam, M.M., Chowdhury, M.A., Sayeed, M.A., Hossain, E.A., Ahmed, S.S., Siddique, A.: Finite element analysis of steel fiber-reinforced concrete (SFRC): validation of experimental tensile capacity of dog-bone specimens, *International Journal of Advanced Structural Engineering*, (2014), pp. 6-63
- [59] Egyptian Code ECP203-2007: Design and Construction for Reinforced Concrete Structures, Research Centre for Houses Building and Physical Planning, Cairo, Egypt.
- [60] Elstner, R.C., Hognestad, E.: Publications 30-1, International Association for bridges and structural engineering, 1956.
- [61] Egyptian Code ECP 208-2005: Practice for the Use of Fiber Reinforced Polymer (FRP) in the Construction Fields, Egyptian Ministry of Housing, Utilities, and Urban Development, Egyptian Housing and Building National Research Center, 2005., pp. 160
- [62] Ivanco, V.: NonLinear Finite Element Analysis, PhD Theises, Faculty of Mechanical Engineering, Technical University of Kosice, Slovakia, 2011.